THESIS

THE DXO DECAPPING EXONUCLEASE IS A RESTRICTION FACTOR FOR RNA VIRUSES

Submitted by

Erin R. Lynch

Graduate Degree Program in Cell and Molecular Biology

In partial fulfillment of the requirements

For the Degree of Master of Science

Colorado State University

Fort Collins, Colorado

Fall 2019

Master's Committee:

Advisor: Brian Geiss

Jeffrey Wilusz
Rushika Perera
Tim Stasevich

ABSTRACT

THE DXO DECAPPING EXONUCLEASE IS A RESTRICTION FACTOR FOR RNA VIRUSES

Cellular RNA exonucleases, such as XRN1 and DXO, aid in the destruction of defective cellular mRNAs and help maintain overall cellular health. The RNA decay system, however, also serves another purpose – degrading viral RNAs. The XRN1 exonuclease is known to be a major antagonist of RNA virus genomes, but the role of other cellular RNA decay enzymes in controlling viral infection is less clear. The cellular 5' decapping exonuclease DXO is able to recognize, de-cap, and degrade RNAs lacking 2'-O-methylation on the first nucleotide after the 5' cap, helping the cell to discriminate self from non-self RNAs. Preliminary data we have developed indicate that flaviviruses and alphaviruses replicate to much higher levels in DXO deficient cells than in cells containing DXO, indicating that DXO may also act as a cellular viral restriction factor. Interestingly, flavivirus genomes contain a 5' cap that is generally 2'-O-methylated at the first base of the transcript, providing a potential mechanism to evade DXO degradation. Overall, our results indicate that the DXO decapping exonuclease helps control the replication of positive strand RNA viruses in cells and represents a new viral restriction factor.

ACKNOWLEDGEMENTS

I would like to thank my advisor, Brian Geiss, for all of the support and guidance he has provided me. With his extensive knowledge, encouragement, and positivity, I am proud of the thesis I have completed and the scientist I have become. I would also like to thank the Geiss Lab's former and current members for their support and assistance. Thank you to Kristen Feibelman, Jessie Filer, and Kelly Du Pont for teaching me various techniques in virology and biochemistry that made my research possible. I want to thank Davis Moline for being the best mentee a graduate student could ask for and being patient as I learned how to be a mentor.

Thank you to the lab of Dr. Jeff Wilusz for teaching me techniques in RNA biology. Without the assistance and advice from Dr. Jeff Wilusz, Dr. Joe Russo, Dr. Dan Michalski, and Dr. Phillida Charley, all of my RNA would be degraded. Also thank you to my committee members for all of their feedback and dealing with my endless Doodle Polls.

A special thanks to my parents, Lori and Jim Lynch, and my sister, Olivia, for always being there for me and supporting me during my pursuit of a graduate degree. You have all been a source of constant encouragement and advice even on the toughest days.

Thank you to my wonderful boyfriend, Tyler Neavin, for the continuous supply of optimism, encouragement, and motivation. Also thank you to our dog, Millie, for the constant laughs and unconditional love. You are my rocks and I am so lucky to have you both in my life.

TABLE OF CONTENTS

LIST OF FIGURES

Introduction

Flaviviruses and Alphaviruses: A Global Health Problem

Viruses that fall under the alphavirus and flavivirus genera continue to be a major health threat across the globe. Approximately thirty-five of the seventy known flaviviruses are associated with disease in humans and an estimated two-thirds of the world's population is affected by such viruses[1]. Transmitted primarily through mosquitoes, these viruses are highly prevalent in the tropics and underdeveloped countries. Due to the significantly high number of infections, the costs of health services as well as to the economies of affected countries have increased substantially. Those living in impoverished countries are more susceptible to flaviviruses and alphaviruses due to poorer living conditions and insufficient access to treatment. Flavivirus disease can cause serious morbidity and mortality in afflicted areas, and these viruses represent a serious global health concern.

Dengue virus (DENV), known to cause the disease "break-bone fever", is one of the most prevalent of the flaviviruses with over one-third of the world's population at risk of infection[2]. Dengue viruses are transmitted by *Aedes aegypti* mosquitoes, which are relevantly wide-spread geographically[3]. There are four separate serotypes of DENV that co-circulate, each causing a range of symptoms and disease[3]. The majority of infections are asymptomatic or cause mild disease such as fever but those who experience a secondary DENV infection increase their risk of developing more severe disease such as hemorrhagic fever or dengue shock syndrome[3]. There is no cross-protection between serotypes, and when the host immune system is primed against one DENV serotype, subsequent DENV infections with different serotypes leads to worse disease via a process known as antibody-dependent enhancement (ADE) [4,5]. ADE can lead to dengue shock syndrome and dengue hemorrhagic fever, both of which have high mortality rates.

Making a vaccine against DENV has shown to be difficult as it needs to protect against all four serotypes without leading to ADE, resulting in very slow development of safe and effective vaccines against these serious pathogens.

Zika virus (ZIKV) first emerged as an epidemic in 2015 in Brazil and caused panic as disease such as microcephaly in babies and Guillain-Barre syndrome in adults were linked to infections[6,7]. ZIKV was shown to be spreading through the Americas with a few cases being reported in Africa and Asia. ZIKV is transmitted through the *A. aegypti* mosquito and can then be transmitted from mother to fetus. The most common symptoms associated with ZIKV are nonspecific diseases such as a fever or rash and diagnostics specific to ZIKV are not available in lesser-developed countries[8]. Mechanisms behind ZIKV infections are still not well-understood as there continues to be a need for effective antiviral therapeutics as well as cheaper and easier to use diagnostic tools.

Yellow fever virus (YFV) has re-emerged within the last several years as a health threat in South America and central Africa. Yellow fever virus was first identified in Africa and introduced to the Americas during the 15th or 16th century[9]. Approximately 200,000 cases of YFV arise every year with 15% of infections leading to death[10]. YFV can lead to lesions of the liver, kidney, or heart and with more serious infections, death[11]. There are vaccines available against YFV however they are not easily accessible in underdeveloped countries. Approximately 393 to 427 million people living in YFV risk zones are still in need vaccinations in order for 80% of the population to be covered[12]. Due to the most recent outbreaks in countries such as Brazil and Nigeria, there is a need for further elucidation of YFV replication to learn how to contain and prevent the virus more effectively.

One flavivirus that continues to cause problems within the United States and Canada is West Nile Virus (WNV). WNV is transmitted by *Culex* mosquitoes and is maintained in nature by cycling through birds and mosquitoes[13,14]. Once infected, WNV replicates within multiple tissues including in the brain. WNV can cause a variety of flu-like symptoms including fever, rash, and even vomiting while less than one percent experience neuroinvasive disease[15]. Currently there are no vaccines or therapeutic antivirals available for WNV and prevention relies on managing mosquito populations or using insect repellent. WNV is one the largest arboviral outbreaks recorded in the U.S. and the highest number of infections are found in the Midwest during the Summer[15]. While surveillance of mosquitoes and WNV incidents in the community can help contain an outbreak, development of a vaccine would be much more effective.

Similar to flaviviruses, alphaviruses are mosquito-transmitted arboviruses that pose a threat worldwide. Chikungunya virus (CHIKV) is the main example of a globally-relevant alphavirus. The word Chikungunya comes from East Africa and means "that which bends up" due to the severe joint pain and swelling the virus induces along with a fever and rash[16]. One of the first CHIKV cases was reported in 1952 in Tanzania and has since spread throughout Africa, Asia, Europe, and the Americas[16,17]. Various pain medications can be administered to patients experiencing severe joint pain but no vaccines or therapeutic treatments have been approved for human use[18]. CHIKV is commonly spread through the *A. aegypti* mosquito found primarily in tropical and subtropical regions[19]. More recently the virus has evolved to replicate in other mosquitoes such as *Aedes albopictus* thus allowing it to spread past these tropical regions into more temperate locations, significantly increasing the number of those at risk of infection[19].

An alphavirus that could cause the next major outbreak is Mayaro virus (MAYV). MAYV is commonly mistaken for CHIKV as it causes a fever as well as severe joint pain and

swelling[20]. Severe infections lead can lead to hemorrhage, inflammation of the heart muscle, and death[21]. MAYV circulates between *Hemagogus janthinomys* mosquitoes and non-human primates[21]. The virus is primarily found in neotropical cities and has been isolated from mosquitoes, humans, lizards, and birds[22]. Currently only a few minor outbreaks have been recorded but there is a continuous increase in infections reported in Brazil[20]. To further understand MAYV on a molecular level may aid in containing any future outbreak.

Unlike other alphaviruses discussed, Venezuelan Equine encephalitis virus (VEEV) not only can cause outbreaks but can also be used as a biological warfare agent when aerosolized[23]. As the name suggests the virus causes severe encephalitis and replicates within the lymph nodes, heart, lung, kidney and pancreas[24]. IA/B, IC, ID, and IE are the four antigenic varieties of VEEV but are indistinguishable from one another[23]. The virus can be maintained in nature by circulating through rodents and mosquitoes while the cause outbreaks in humans and horses[23]. VEEV has been reported in North, Central, and South America while both the U.S. and the former Soviet Union has developed a biological weapon from the virus[25]. Vaccines against VEEV is crucial for protection from outbreaks and attacks using the virus as a weapon. The vaccine must provide protection at differing routes of infection both subcutaneous and aerosol to be the most effective.

Each of these aforementioned viruses cause significant human disease, but there is a general lack of effective vaccines and antivirals to treat infections. Developing a better understanding of how these viruses replicate and interact with the cell will help in the development of these therapies and may help to save lives. Since the occurrence of various viral outbreaks such as those mentioned, flavivirus and alphavirus research has advanced substantially. Despite being from different viral families and having a few minor genomic

differences, flaviviruses and alphaviruses share many similarities between their replication cycles. The infection begins when a virus attaches to a cell and undergoes receptor-mediated endocytosis. In the endosome, acidification occurs and triggers a conformational change in the viral glycoproteins that allow fusing of viral and cellular membranes[26,27]. This conformational change allows the virus to fuse its viral envelope to the endosomal membrane and release the viral RNA into the cytoplasm.

Flavivirus genomes contain a 5' cap that is N7-methylated as well as a 2'-O-methylated first base of the transcript and a stem loop structure at the 3' end to terminate translation shown in Figure 1. Alphaviruses also contain a 5' cap that is N7 but not 2'-O-methylated and a 3' poly(A) tail. With the proper 5' and 3' molecular structures and modifications, the virus genomes resemble mRNA and can replicate using cellular translation machinery directly in the cytoplasm without further modifications. Flavivirus genomes are organized to express structural proteins at the 5' end and nonstructural proteins at the 3' end[28]. The nonstructural and structural proteins are translated into a single polyprotein before being translocated across the ER membrane. Viral and cellular proteases cleave the polyprotein into individual proteins where they can be modified in

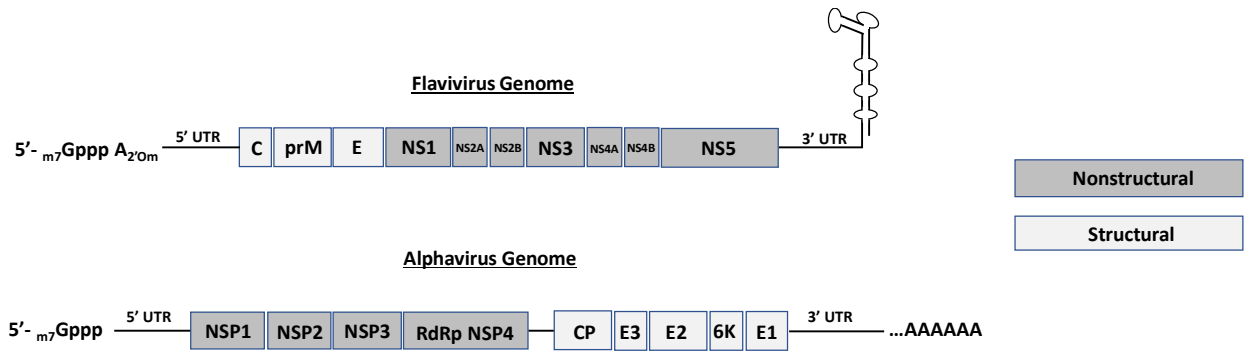

Figure 1. Flavivirus and Alphavirus genomic structures.

the ER. Following translation, nonstructural proteins such as NS3 and NS5 in flaviviruses

replicate the viral genome while structural proteins begin to form the packaging for viral genomes[26,27]. Replication of flavivirus genomes and particle assembly occurs in vesicles located in the lumen of the ER[28]. Structural proteins such as capsid (C), pre-membrane (prM), and envelope (E) must undergo modifications in preparation for viral particle budding[29]. Once a particle buds from the ER, maturation must occur in the Golgi complex and prM is cleaved by furin protease. Cleavage of prM is crucial for the rearrangement of E proteins on the virion surface and maturation of the particle[28,29]. The matured viral particle buds from the Golgi and fuses with the cellular membrane through the structural proteins on the viral surface thus allowing viral budding from the cell[29].

Alphaviruses express a nonstructural polyprotein at the 5' end and a structural polyprotein at the 3' end[28]. During the early stage of translation the nonstructural polyprotein, P123, in the alphavirus genome is translated first. P123 is cleaved by the viral nsP2 protease and form a complex necessary for further viral genome replication as well as translation of structural polyproteins. Like flaviviruses, alphavirus polyproteins undergo cleavage by viral and cellular proteases and non-structural proteins are processed in the ER to form functional proteins[26,27]. The nonstructural protein, nsp4, replicates the viral genome that is packaged in a nucleocapsid[26,27]. During alphavirus genome packaging, structural glycoproteins such as PE2-E1 that form the spike complex undergo processing in the ER and Golgi apparatus[28,30]. Genomic RNA is subsequently packaged into capsids made up of capsid protein and trafficked to the plasma membrane for budding. The spike complex is transported to the plasma membrane where it is activated by the cellular furin protease and allows budding of the assembled alphavirus particle to occur[28]. Once a virus buds from the cell, the infectious particle is free to infect adjacent cells.

One of the challenges for cells is to detect and destroy viral genomes during infections, which can be difficult when viral genomes look similar to cellular RNAs. Cellular mRNAs contain a 5' 7-methylguanosine cap that is 2'-O-methylated and a 3' poly-A tail which are all necessary for RNA transport, processing, and translation. Any RNAs that do not contain the appropriate modifications are recognized as defective and are degraded by the cellular RNA decay machinery[31]. The single-strand positive sense alphavirus and flavivirus genomes also contain a 5' cap that is 2'-O-methylated in flaviviruses but not alphaviruses[27,32]. In addition, flaviviruses do not contain a 3' poly(A) tail but instead terminate with a stem loop structure while alphaviruses do contain the appropriate 3' poly(A) tail[1]. The genomes contain the necessary molecular features to be translated by the cell, however, they appear as defective mRNAs to the cellular RNA decay machinery due to missing cellular markers such as a ribose methylation or a poly(A) tail. With the decay machinery unable to recognize the viral RNA as self, it is likely targeted for degradation, making this pathway the cell's first line of defense against infection.

The Cellular RNA Decay Pathway

Cellular RNA decay pathways regulate gene expressions through maintaining appropriate levels of mRNA transcripts to undergo translation and degrade faulty RNAs[33]. In order to sustain equilibrium, the cell must respond quickly to both internal and external cues through changing the abundance of mRNAs to be translated[33,34]. Each mRNA transcript is equipped with a 5' cap and poly(A) tail to protect against degradation, however, these modifications are thoroughly scrutinized through a series of protein-protein and protein-RNA interactions. As the poly(A) tail undergoes a sufficient amount of deadenylation or the 5' cap contains inadequate methylation,

these transcripts become susceptible to degradation. By degrading defective RNAs, the cell is protected against aberrant mutations or deletions that can have fatal downstream effects.

To initiate the degradation of a specific transcript, deadenylation must first occur. The PAN2-PAN3 (PAN2/3) deadenylation complex catalyzes this process by deadenylating tails longer than approximately 150 bp until the CCR4-NOT (CNOT) deadenylation complex steps in to finish the job[35]. The PAN2/3 complex does not affect stability of the transcript and acts as a preliminary step[36,37]. Poly(A) binding proteins (PABP) bind to the poly(A) tail to increase transcript stability and prevent deadenylation of the tail[38,39]. The catalytic subunit of CNOT, CAF1, deadenylates unbound poly(A) tail until it becomes blocked by a PABP. Upon CAF1 stalling, the CCR4 catalytic subunit of CNOT becomes activated by the PABP and removes the RNA binding protein as it continues deadenylating[39]. The deadenylated transcript is subsequently uridylated by terminal uridylyltransferases (TUTases), promoting decapping and degradation of the transcript[38,40].

The 5' cap provides mRNA transcripts the ability to undergo translocatation with the help of cellular factors from the nucleus to cytoplasm for translation, increases splicing efficiency, and protects from 5' to 3' exoribonucleases[41]. Removal of the 5' cap via decapping enzymes plays a significant role in downstream expression of the transcript by marking it for decay[41,42]. The well-studied decapping enzyme DCP2 is responsible for removing the α- and β- phosphate of the cap and generating a monophosphorylated RNA transcript, a perfect substrate for a 5' to 3' exoribonuclease[43]. For DCP2 to be activated and target a transcript, there are a variety of cofactors that need to be present. For instance, the LSM1-7 complex binds to the deadenylated RNA and recruits DCP2 while the RNA helicase, DDX6, reassembles the transcript for optimal binding of proteins[44,45]. DCP2 was initially thought to be the primary decapping enzyme in

eukaryotes but was found to only affect a subset of transcripts[42]. Recent studies have shown other proteins possessing similar decapping activities such as the Nudix proteins, Nudt16 and Nudt3, and DXO[46–48]. Like DCP2, the Nudix proteins prefer a subset of transcripts while DXO targets transcripts with an incomplete 5' cap[47,49]. Nonetheless, there are many more decapping enzymes to be discovered, most of which are suspected to be a part of the Nudix family. With the 5' cap removed and a monophosphorylated transcript remaining, 5' to 3' or 3' to 5' exoribonucleases can begin to degrade the target mRNA.

While deadenylation and decapping are an efficient and more common means of marking a transcript for exonucleolytic decay, endonuclease activity can also lead to the same result. During active translation of an mRNA by ribosomes, endonucleases target a sequence or structure within the transcript for cleavage[50,51]. Once cleaved into smaller fragments, the RNA can be further degraded by 5' to 3' or 3' to 5' exonucleases[52]. There are multiple endonucleases associated with the polysome and RNA decay, such as PRM-1. Like other decay pathways, endonucleases are thoroughly regulated to prevent unwanted nucleolytic decay. For instance, PRM-1 must undergo phosphorylation by the tyrosine-protein kinase, Src (c-Src) to be targeted to the polysome and activated for endonucleolytic decay[50]. Hyperphosphorylation of serine residues on the endonuclease, GB3P, is imperative for its activity[53]. In addition to protein modifications, endonucleases such as Argonaute2 (Ago2) may be activated through the RNA interference (RNAi) pathway[54]. Through microRNAs and small interfering RNAs (siRNAs) produced by the dicer protein, Ago2 is guided to a target mRNA for subsequent cleavage[55]. This cleavage event leads to additional degradation by exonucleases.

With the 3' end of a transcript exposed after deadenylation, 3' to 5' exoribonucleases can target the RNA for degradation. In eukaryotes, the major 3' to 5' ribonuclease is the RNA

exosome complex[56]. The multisubunit complex is recruited to the unprotected 3' end of transcript through the RNA-induced silencing complex (RISC) after the RNA has undergone endonucleolytic cleavage by Ago2[56,57]. The RNA exosome complex may also be recruited to a target transcript through the cofactor SKI7[58]. SKI7 bridges the exosome to ski complexes and serves a role in nonstop decay by eliminating defective transcripts such as those containing aberrant translation termination[58]. An additional major player of 3' to 5' decay is the exoribonuclease, DIS3L2. After deadenylation as discussed above, TUTases polyuridylate the 3' ends and create an optimal substrate for DIS3L2[59]. The ribonuclease is also shown to play a role in apoptosis as well as cell differentiation[59]. The dysregulation of 3' to 5' decay leads to serious disease such as Perlman syndrome and kidney cancer primarily in children with DS3L2 mutations[59].

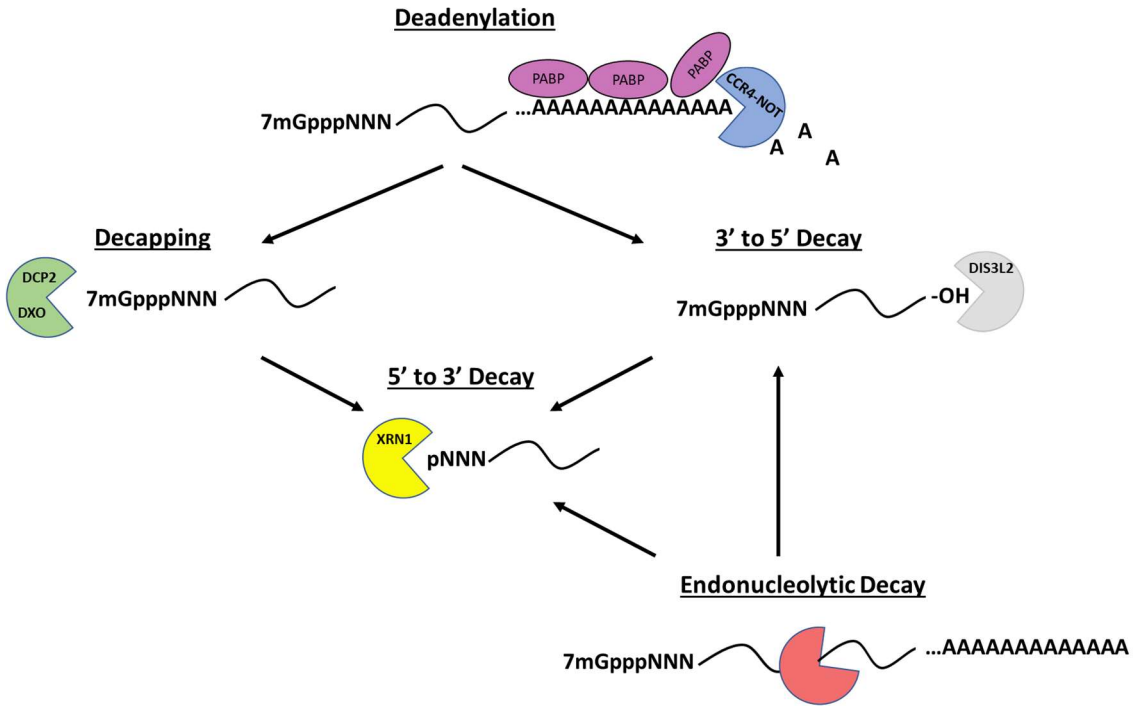

Figure 2. Simplified diagram of RNA decay pathways.

Following decapping of the 5' end, a transcript can now act as a substrate for 5' to 3' exonucleolytic decay. This pathway is primarily accomplished by the well-studied exoribonuclease, XRN1. XRN1 is a processive ribonuclease that favors RNAs containing a monophosphate on the 5' end after decapping or endonucleolytic cleavage as described above[60]. It has been reported that XRN1 serves as a buffer for synthesis and degradation of mRNAs, thus suggesting the ribonuclease greatly contributes to regulating gene expression[61,62].

The Evolutionary Warfare Between Flaviviruses and Cellular RNA Decay

The cell is well-equipped with a variety of antiviral proteins and pathways to overcome viral infections. Over time, viral proteins have evolved mechanisms of antagonizing these immune responses. For instance, NS5 in flaviviruses and nsP2 in alphaviruses are both nonstructural proteins that inhibit JAK-STAT signaling and thus inhibit host type-1 interferon (IFN-1) responses[32,63]. Flavivirus proteins have also been shown to inhibit molecules crucial to pattern recognition receptor (PRR) signaling. The E protein of WNV targets a major activator of Nf-κB signaling thus impairing IFN-1 induction and pro-inflammatory cytokines[64]. With the interferon response down, viruses can replicate more efficiently. Altogether, alphaviruses and flaviviruses have the ability to subvert the innate immune response. There is, however, another way to surpass antiviral pathways and that requires a disguise.

While the normal function of the RNA decay pathway is to make sure that cellular mRNAs are undamaged and of high quality, this pathway has a second function: antiviral defense. During flavivirus infections after viral genomes are released into the cytoplasm for translation, the defective mRNA-looking transcripts are quickly noticed by the cellular RNA decay pathway. Seemingly, the viral RNAs have no chance against the key players of RNA decay as previously mentioned. However, flaviviruses have evolved to contain tricks up their

genomes called, subgenomic flavivirus RNA (sfRNA). Upon 5' to 3' decay by XRN1, the ribonuclease stalls on pseudoknot-like structures in the flavivirus 3' untranslated region (UTR) of the genome[65]. Consequently, XRN1 activity is repressed, causing increased half-lives of uncapped RNAs, both cellular and viral, and dysregulation of the decay pathway while giving viral RNAs a chance to continue replicating[65,66]. It is hypothesized that sfRNA may act as decoys for factors of the decay pathway in humans and RNAi in mosquitoes allowing viral genomes to evade degradation, thus aiding in their replication[67]. SfRNA has also been shown to bind factors of innate type I interferon (IFN) response such as RIG-I and therefore suppressing both the protein and its associated IFN pathway[68]. It can also interact with the cellular proteins G3BP1, G3BP2, and CAPRIN that are involved in translating IFN-induced mRNAs[69]. Current research shows sfRNA is able to act as a "protein sponge" and sequester a variety of factors involved in RNAi and splicing, thus suppressing these crucial cellular pathways[69]. SfRNA plays various roles within the cell, affecting multiple pathways leading to dysregulation of crucial activities. Overall, sfRNAs formed during flavivirus infection have been shown to be critical in providing an optimal environment for viral replication and contributes significantly to the pathogenesis observed with these viruses. However, most of the studies to date have focused on the role of XRN1 in flavivirus infections, and little to no work has been done examining the roles of other components on restricting flavivirus infections.

Flaviviruses genomes are not the only viruses to have a way of antagonizing the immune response. Alphavirus 5' and 3' UTRs aid in increasing virulence and evading IFN responses. In the 5' UTR, studies show that a single point mutation changing G to A at the third nucleotide of VEEV causes the virus to lose virulence in mice[24,70]. The mutated virus was shown to be more susceptible to IFN-α/β responses compared to the wildtype virus, thus leading to attenuation in

the mutant virus and suggesting the 5' UTR plays a crucial role in viral evasion of host immunity by inhibiting binding of IFN- α/β factors[70]. In addition, alphaviruses contain a 5' cap but lack 2'-O-methylation, making it a target for the IFN-stimulated gene, IFIT-1[71]. Instead of self-methylating or stealing caps from host mRNAs, alphaviruses inhibit the binding of Ifit-1 by containing a thermodynamically stable stem loop structure at the 5' end[30]. Mutations to this stem-loop creating a less stable structure increases the RNA's susceptibility to Ifit-1[30]. At the other end of the alphavirus genome, the 3' UTR can bind cellular proteins such as HuR. By binding HuR with a high affinity, the protein prevents deadenylation and subsequent RNA decay[72]. The 3' UTR also acts as a protein sponge, similar to the sfRNA previously described, and sequesters HuR leading to massive dysregulation of gene expression[73]. Overall, the 5' and 3' UTRs significantly affect viral replication however there are difference in structures and functions between alphaviruses and flaviviruses.

Is DXO is a restriction factor for RNA viruses?

As flaviviruses and alphaviruses have evolved to evade or suppress cellular decay pathways and immune responses, cells have also developed methods to fight back. Here, we look at the decapping 5' to 3' ribonuclease, DXO, and its role in the antiviral response. Unlike XRN1, DXO utilizes capped 5' ends as substrates and targets incompletely methylated 5' caps[42,48]. DXO has the ability to decap the RNA substrate and subsequently degrade the transcript 5' to 3'[42,48]. One study shows 2'-O-methylation of the 5' cap protects RNAs from DXO activity[74]. As previously mentioned, flaviviruses contain a 2'-O-methylated 5' cap which may be a method of evading DXO degradation. Interestingly, alphaviruses do not contain 2'-O-methylated caps causing question as to how they escape degradation by DXO.

The role of DXO in viral infections has never been studied, so it is currently unknown of DXO would play a role in viral infection. Therefore, the focus of this thesis is to begin defining if and how DXO influences flavivirus and alphavirus infection. Previous research has shown that DXO is a nuclear protein in HeLa and U2OS cell lines but it is unknown where DXO is localized within HEK cells[47,75]. Our studies have shown that DXO is a cytoplasmic protein in HEK cells and therefore co-localizes with viral RNAs. We first examined role DXO plays in flavivirus replication through analyzing viral RNA abundance and growth kinetics in wildtype (WT) and DXO CRISPR knockout (DXO KO) cell lines. Results showed a significant increase in viral replication and cytopathic effect in some viruses but not others thus indicating not all viruses are affected by DXO. We also observed the effect of DXO on a positive strand RNA virus from a different genus, SINV. Results show a significant increase in overall titer and viral RNA abundance in the absence of DXO compared to WT cells. We further examined DXO on a biochemical level to test if the exonuclease is inhibited by specialized RNA structures like XRN1. Recombinant DXO was added to radiolabeled 3' UTR's of DENV and Rift Valley fever virus (RVFV). Our data indicates that DXO does not create decay intermediates such as sfRNAs after degrading the DENV 3' UTR. This data suggests the ribonuclease, unlike XRN1, can decay the highly structured 3' UTRs without stalling. Overall, our results suggest that DXO does not play the same role in controlling viral replication of different viruses regardless of being in the same genus. The decapping exonuclease is shown to control the replication of positive strand RNA viruses in the cells and represents a new viral restriction factor. Further elucidation of mechanisms behind DXO activity during viral infections is necessary to shed light on how DXO targets viral RNAs and why the decapping exonuclease affects certain viruses but not others.

Materials and Methods

Cells and viruses.

Wildtype (WT) and DXO-knockout (DXO-) human embryonic kidney (HEK) 293T cells were generously provided by Dr. Megerditch Kiledjian at Rutgers University while Vero cells were purchased from ATCC. DMEM medium (Thermo Fisher Scientific) with the addition of 2.5 mM HEPES, 10% fetal bovine serum, and penicillin/streptomycin was used to culture the cells. Cells were propagated at 37˚C in 5% CO_2.

SINV (TE3'2J), WNV (subtype Kunjin, strain FLSDX), YFV (strain 17D), and ZIKV (strain PRVABC59) were used in this study. To produce the Kunjin E218A mutant, a novel virus launch system was used. Briefly, PCR fragments containing the Cytomegelovirus (CMV) immediate early promoter (612 bp, fragment #1), the 5' region of the Kunjin virus genome (8354 bp, fragment #2), and the 3' end of the Kunjin virus genome containing a Hepatitis Delta virus ribozyme (2822 bp, fragment #3) were produced using the New England Biolabs Q5 DNA polymerase system according to the manufacturer's instructions[76]. PCR primer sequences for each fragment were:

<u>Fragment #1 (CMV)</u>

Forward: 5'- tctatcggaaGATTATTGACTAGTTATTAATAGTAATCAATTACG

Reverse: 5'- gcgaactactCGGTTCACTAAACGAGCTC

<u>Fragment #2 (5' KUNV)</u>

Forward: 5'- tagtgaaccgAGTAGTTCGCCTGTGTGAG

Reverse (E218A mutation): 5'- cccaatacatGGCATGTGTGGAATTCCG

Fragment #3 (5’ KUNV)

Forward (E218A mutation): 5’- cacacatgccATGTATTGGGTGAGTCGAG

Reverse: 5’- gtcaataatcTTCCGATAGAGAATCGAG

The E218A mutation was engineered into the Fragment #2 reverse primer and Fragment #3 forward primer and mutant fragments were also produced. PCR products were gel extracted with the Qiagen Gel Extraction kit and quantified by UV spectrophotometry and agarose gel electrophoresis. To assemble the WT or E218A fragments, equal molar amounts of each fragment were mixed in a total DNA mass of 200ng for each virus in ultrapure water in a final volume of 15µl. An equal volume of New England Biolabs NEBuilder 2X Master Mix was added to the DNAs, and the reaction was incubated at 50ºC for 4 hrs. To produce virus from the assembled DNAs, the assembled DNAs were transfected directly into Vero cells by adding 1µl of JetPrime transfection reagent to the assembly mixture, incubating at 22oC for 15 minutes, and adding the transfection mixture to 50% confluent Vero cells. cDMEM media was changed 24 hrs after transfection, and the cells were incubated for 6 additional days and monitored for cytopathic effect. Media was collected on day 6 as the P0 stock. Virus was amplified in a larger culture for 7 additional days and collected as the P1 stock. Finally, the P1 stock was used to infect a T150 flask of 50% confluent Vero cells for 7 days, media was collected and clarified of cellular debris, and clarified media frozen at -80ºC as the P2 stock. The P2 stock was quantified for infectivity via focus forming assay, and the presence of the E218A mutation was verified by extracting RNA from the P2 stock, reverse transcribing and PCR amplifying the NS5 region of Kunjin virus using primers 5’GTTTATCCATAACATGGACTCTTGT and

5’GTAGAGGTTTTCCCACTGCTCT, and the sequence of the PCR amplicon determine by Sanger sequencing.

Viral stocks were grown on Vero cells for several days until significant cytopathic effect was observed. Media was collected and centrifuged at 19,000 x g for 10 minutes to pellet cell debris. Virus-containing media was then aliquoted and stored at -80˚C. Viral titers were obtained through plaque and focus forming assays.

Nuclear-Cytoplasmic Fractionation and Western Blots

Cells were plated in 10 cm plate at 20% confluency and incubated overnight. Media was removed from plates and gently washed with 1XPBS. Cells were trypsinized and trypsin was diluted by adding equal volume DMEM. Cells were thoroughly mixed then pelleted at 300 x g for 5 minutes. Supernatant was discarded without disturbing the cell pellet. Cells were resuspended in 2 mL 1XPBS and re-pelleted under same conditions to ensure excess media is removed. Supernatant was discarded and cell pellet was resuspended in 1 mL NP-40 lysis buffer [0.5% NP-40, 10 mM Tris HCl pH 8.5, 1.5 mM $MgCl_2$, 10 mM EDTA, 140 mM NaCl]. Suspended cells were transferred to a 1.7 mL Eppendorf tube and incubated on ice for 10 minutes. Some of the whole cell lysate was saved as a control and set aside. Lysed cells were centrifuged at 500 x g for 5 minutes at 4˚C. Supernatant was saved as cytoplasmic fractions and stored on ice. The pellet containing nuclear fractionation was with NP-40 lysis buffer with inversion mixing and re-centrifugation at 500 x g. Supernatant was discarded and nuclear pellet was resuspended in 500 μL H_2O. Samples can be stored at -20˚C or used immediately for western blotting.

Cytoplasmic and nuclear fractions were resolved on a 12% polyacrylamide SDS-PAGE gel for one hour at 120 V. Proteins were transferred to PVDF (Immobilin-P #IPVH0010) for one

hour at 100 V using Bio-Rad's Mini Trans-Blot Cell system (#1703930) and 1X transfer buffer [25 mM Tris, 192 mM glycine, 10% methanol]. Blots were blocked with 2% non-fat dry milk in TBS-T for thirty minutes. Primary antibodies were added to the blocking buffer at appropriate dilutions and incubated on a rocker at 4 ˚C overnight (see Table 1 for antibody details). Blots were washed in 5 times in TBS-T for 5 minutes each wash. Blocking buffer with appropriate secondary antibody was added to the blot and incubated at room temperature for one hour. Wash steps were repeated. Blots were developed with SuperSignal West Dura Extended Duration Substrate using protocol (Thermo Scientific #34075). Images of blots were taken using the Biomolecular Imager from Azure Biosystems.

WT vs. DXO- HEK Cell Growth Curve

WT and DXO- HEK cells were plated at 20% confluency in 12-well plates. Plates were incubated in optimal conditions previously mentioned and counted every 12 h for 72 h. Cells were trypsinized and diluted in Trypan Blue (Corning #25-900-CI). Live cells were counted using a hemocytometer and plotted using GraphPad Prism 8.

Viral Infections.

For analysis of intracellular viral RNA abundance, 10 cm plates were seeded to 20% confluency with WT or DXO KO cells. The cells were infected with ZIKV at an MOI of 1 and incubated at 37˚C for 72 h. Media was discarded and 4 mL of Trizol (ThermoFisher Scientific) was added directly to the cells. Total RNA was extracted following the manufacture's protocol and analyzed by digital PCR.

SINV, WNV (subtype Kunjin), and YFV were used to infect WT and DXO- HEK 293T cells at a MOI of .01. SINV was incubated on the cells at 37˚C for 72 h. Virus-containing media

and cells were collected and stored in aliquots at -80˚C after 4, 8, 12, 24, 36, 48, 60, and 72 h post-infection. KUNV and YFV were incubated on the cells for seven days, collecting infectious media and cells every 24 h.

Viral Titer Quantification by Focus Forming and Plaque Assay.

Flavivirus titers for YFV, ZIKV, and WNV growth curves were quantified from media by focus-forming assay, as previously described[77]. DENV titers were quantified using a plaque assay. Baby hamster kidney (BHK) cells were used to seed 6-well plates at 90 to 95% confluency. Serial dilutions of infectious DENV media were made in PBS containing 1% 100X Ca^{2+}, Mg^{2+} ions and 10% FBS. Media was aspirated from BHK cells and 250 μL of each virus dilution was added to individual wells. Cells were incubated with diluted virus for one hour at room temperature on a rocker. 3 mL of an overlay containing equal volume sterile 2% agarose and 2X DMEM was added to each well. Once solidified, the plates were incubated for five days at 37˚C. 1 mL of 10% DMEM was added after two days of incubation to prevent cells from drying out. Plaques were stained overnight at 37˚C using 2 mL per well of 1:12 Neutral Red to PBS.

Sindbis virus titers were quantified by plaque assay. 24-well plates were seeded with Vero cells and incubated overnight to achieve full confluency. Infectious media for Sindbis growth curve were serially diluted 10-fold and incubated on the Vero cells for 1 h at 37˚C. An overlay of an agarose-DMEM mixture [DMEM powder (Sigma-Aldrich), penicillin/streptomycin, 10% FBS, 4% NaHCO3] was added on top of cells and virus. The plates were incubated for 72 h at 37˚C. Cells were fixed with 10% formaldehyde before agarose-DMEM was removed from wells. Cells were washed with PBS and stained with .1% crystal

violet (Sigma-Aldrich) for 10 min. Plaques were counted and calculated for each timepoint and reported as pfu/mL.

In Vitro Transcription of Northern Probes and 3' UTR Substrates

The 3' UTR sequences of ZIKV, DENV, and RVFV were individually cloned into the pGEM4 (Promega) to be subsequently transcribed. The plasmid was transcribed to make the internally radiolabeled Northern probes and 3' UTR substrates by using the SP6 polymerase (ThermoFisher Scientific). 0.5 mM UTP and the addition of α-^{32}P- UTP (800 Ci/mmol). The SP6 protocol was followed and incubated at 37˚C for three hours. The ZIKV 3' UTR probe and radiolabeled 3' UTR substrates underwent cleanup through a denaturing polyacrylamide gel purification. Radiolabeled 3' UTRs were resolved on a 5% polyacrylamide gel containing 7 M urea. Bands were imaged by X-ray film and excised from the gel. Excised desired products were placed in a high salt concentration buffer (HSCB) [400 mM NaCl, 25 mM Tris-HCl pH 7.6, 0.1% SDS] and RNA eluted overnight at room temperature. RNA was purified using a phenol/chloroform isoamyl alcohol (25:24:1) extraction and ethanol precipitation. RNA was resuspended in 20 μL of double distilled H_2O.

Northern Blots

5 μg of total RNA during ZIKV infections was resolved on a 5% denaturing polyacrylamide gel in 1X TBE at 600 V until desired separation has occurred. The RNA was then transferred onto a nylon membrane at 10 V overnight (GE Healthcare #RPN203S) using a wet transfer apparatus at 4˚C. Following the transfer, the membrane was UV-crosslinked using the Stratagene UV Stratalinker Auto-Crosslink function. The membrane was washed using a Northern pre-wash buffer [0.1X SSC, 0.1% SDS] at 60˚C for one hour. The pre-wash buffer was discarded and the membrane was washed in Hybridization buffer [50% formamide, 5X SSC,

1.0% SDS, 0.1 mg/mL salmon sperm DNA, 5X DENHARdTS Reagent] for one hour at 60˚C. The ZIKV 3' UTR Northern probe was added to 25 mL of Hybridization buffer and pre-warmed to 60˚C. Hybridization wash was discarded from the membrane and the Hybridization buffer containing the probe was added. The membrane was incubated with the probe at 60˚C overnight with gentle agitation. The buffer containing the probe was decanted and the membrane was washed twice with Low Stringency Buffer [0.1% SDS, 2X SSC] then twice with High Stringency Buffer [0.1% SDS, 0.2X SSC] for 15 min each at 60˚C. The membrane was subsequently exposed to a phosphor screen for one hour to overnight depending on signal intensity. The membrane was then imaged using the Biomolecular Imager from Azure Biosystems.

Extracellular and Intracellular Viral RNA Quantification.

Extracellular and intracellular total RNA was extracted from using TRIzol reagent (ThermoFisher Scientific) following the manufacturer's protocol. The total RNA was then treated with DNase I (ThermoFisher Scientific) for twenty minutes at 37˚C. Phenol extraction and ethanol precipitation were used to remove DNase I and isolate total RNA. Total RNA quality was assessed using gel electrophoresis to visualize 18S and 28S rRNA to ensure no smearing of bands suggesting RNA degradation.

Viral RNA abundance for Sindbis and West Nile virus was normalized and quantified using digital PCR (dPCR), as described previously [2]. 1 µg of total RNA was reverse transcribed and diluted 1:10 – 1:1000 fold before dPCR for accurate quantification. The following primers were used for dPCR:

Forward GAPDH: 5'- AAGGTGAAGGTCGGAGTCAA

Reverse GAPDH: 5'- AATGAAGGGGTCATTGATGG

Forward ZIKV: 5'- AGGATCATAGGTGATGAAGAAAAGT

Reverse ZIKV: 5 - GCACCAATCTTAATGTTGTCAGG

Forward genomic WNV: 5'- TGGACGGGGAATACCGACTTAGAGG

Reverse genomic WNV: 5'- ACCCCAGCTGCTGCCACCTT

Forward genomic SinV: 5'- CATCGGTGAGAGACCACCTT

Reverse genomic SinV: 5'- AACCACGCCTTTGTTTCATC

Cell Free RNA Decay Assays

Recombinant XRN1 (pET26b-XRN1) and DXO (pET28a-DXO) were transformed into BL21-DE3 cells and purified as previously described[47,78]. For the XRN1 reaction, approximately 200,000 cpm of internally radiolabeled DENV or RVFV 3' UTRs substrates were added to the reaction along with 1 μL Ribolock RNase Inhibitor (ThermoFisher Scientific), 2 μL of 10X NEBuffer 3 (New England Biolabs) and ddH_2O for a final volume of 19 μL. Approximately 0.06 μg of purified XRN1 was added to the reaction. Instead of NEBuffer 3, the DXO RNA decay reaction consisted of 2 μL of 10X IVDA-2 buffer [100 mM Tris-HCl, pH 7.6, 1 M KOAc, 20 mM $MgCl_2$, 0.50 mM $MnCl_2$, 20 mM DTT, and 20 mM spermidine]. Approximately 0.07 μg of recombinant DXO was added. All reactions were incubated at 37˚C. Four timepoints were taken from the reaction and stopped by placing it into HSCB. Phenol/chloroform extraction and ethanol precipitation techniques were used to purify the RNA. The RNA was resolved on a 5% denaturing polyacrylamide gel and exposed to a phosphor screen for one hour to overnight depending on the intensity of the bands. Phosphor screens were subsequently imaged using the Biomolecular Imager from Azure Biosystems.

DXO Over-Expression Cell Line

The p3XFLAG-CMV-10 vector was obtained through Sigma. Mammalian DXO was amplified from HEK cell extracted cDNA using PfuUltra II Fusion High-Fidelity DNA polymerase (Agilent) and the following primers:

DXO Forward +EcoR1 cut site: GATCGAATTCGATCCCAGGGGGACCAAGAG

Reverse DXO +BAMH1 cute site: TCGCGGATCCTATTTGGGAGAGGGAGTCTTGG

Correct PCR product size was confirmed on 1% agarose gel and purified using Wizard SV Gel and PCR Clean-Up System (#A9281). The PCR product and vector were double digested using EcoR1 (NEB #R3101S) and BamH1 (NEB #R0136S). The digest product was then gel purified on a 1% agarose gel using the Wizard SV Gel and PCR Clean-Up System. The DXO insert and vector were ligated using the T4 DNA Ligase (NEB # M0202S). Plasmids were transformed into DH5α cells and plated on LB + ampicillin plates. Plates were incubated at 37˚C overnight. 5 mL LB + ampicillin cultures were grown up overnight using colonies from the plates. Plasmids were miniprepped using the QIAprep Spin Miniprep Kit (Qiagen #27104). Samples were sequenced using Genewiz to confirm plasmids were correct.

Results

DXO is a Cytoplasmic Protein

We first wanted to evaluate if the exonuclease is localized in the cytoplasm where viral RNA is commonly located. Previous data have shown that DXO is a nuclear protein in HeLa cells and U2OS cells but there are no publications regarding DXO localization in HEK cells. WT and DXO KO cells were subjected to nuclear and cytoplasmic fractionation to understand where DXO is localized within the cells. XRN2 and tubulin were used as positive controls and appeared in the nuclear and cytoplasmic fractions, respectively (Figure 3). DXO KO HEK cells were used as a negative control. DXO appeared in the cytoplasmic fraction in WT HEK cells. Based on the conclusion that DXO is co-localized in the cytoplasm with viral RNA, this data suggests that it is

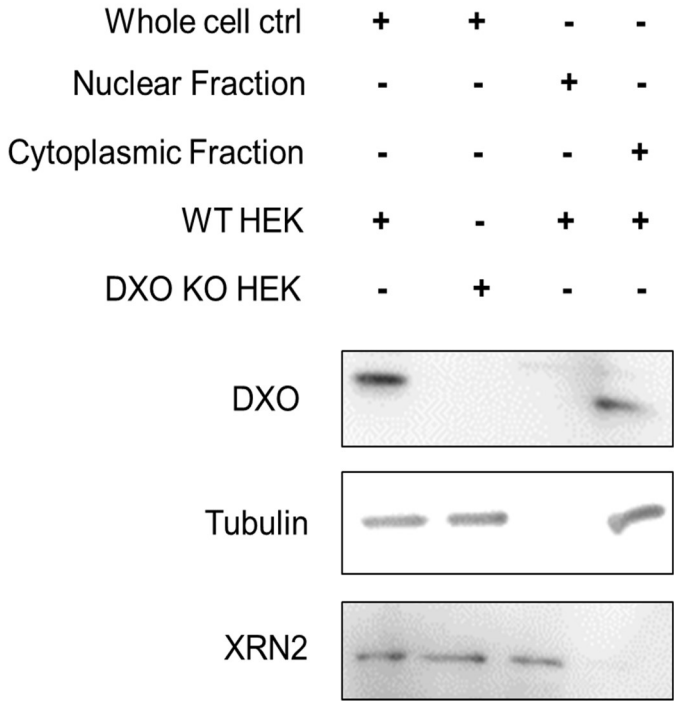

Figure 3. DXO is a cytoplasmic protein in HEK cells. Cytoplasmic and nuclear proteins from HEK cells were fractioned and analyzed via western blotting. Non-fractioned cell lysate (whole cell ctrl) was used as a positive control. Tubulin and XRN2 were positive controls for cytoplasmic and nuclear fractions, respectively. The DXO KO HEK cell line was also analyzed in the set of experiments to show no DXO is present compared to WT cells.

plausible that the 5' to 3' exonuclease plays a direct role in affecting viral replication without needing to re-localize. In addition, we were able to confirm that the DXO KO cell line did not express DXO. This DXO KO cell line along with the WT HEK cells were used in further experiments to study the role of DXO in flavivirus and alphavirus replication.

DXO KO Cells Show a Lag in Replication Rate Compared to WT Cells

Before using DXO KO cells in further experiments, we wanted to understand the differences in growth rates between the wildtype and mutant HEK cells. WT and DXO KO cells were counted over the course of 72 h and compared (Figure 5). Starting at 12 h, there were approximately 1.2-fold more WT cells than DXO KO and 1.7-fold more by 72 h. Overall, linear regression showed a WT growth curve slope of .0136 and .01164 for DXO KO cells. Although DXO KO cells show a delay in growth shortly after being seeded, the CRISPR knockout cell line and WT cells have similar growth rates throughout the rest of the recorded time. Based on this data, it is necessary to consider growth rates when comparing viral titers or abundance of viral RNA. If DXO KO

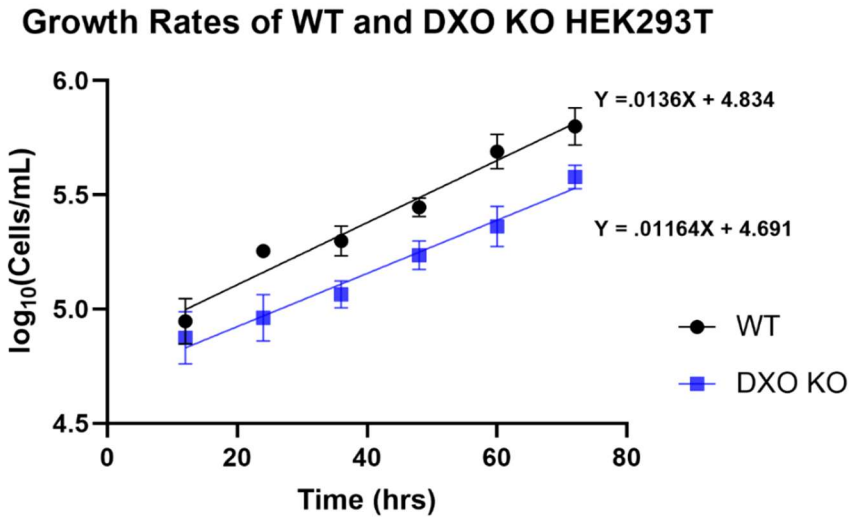

Figure 4. Plot of WT and DXO KO growth rates over 72 h. WT and DXO KO cells were plated in 12-well plates at approximately 20% confluency and counted using Trypan blue every 12 h. Each timepoint contains three replicates. Both cell line growth rates were plotted and compared against each other.

cells take slightly longer to begin replicating at a comparable rate to WT cells, then there will be fewer DXO KO cells at a given timepoint. If we observe an increase in virus replication in DXO KO cells compared to WT cells, then this difference may be even greater when taking cell line replication rates into account.

Cells Lacking DXO Show a Significant Increase in ZIKV RNA Compared to WT Cells

In these studies, we wanted to investigate the effect of DXO on flavivirus replication through analyzing intracellular RNA abundance. WT and DXO KO cells were infected with ZIKV at a MOI of 1.0. Intracellular ZIKV RNA abundance was quantified 72 h after infection of WT and DXO KO cells through extraction and analysis of total RNA by digital droplet PCR. Results showed an approximate 6-fold increase in viral RNA abundance in DXO KO cells compared to WT cells (Figure 6A). This increase in viral RNA abundance was confirmed in a

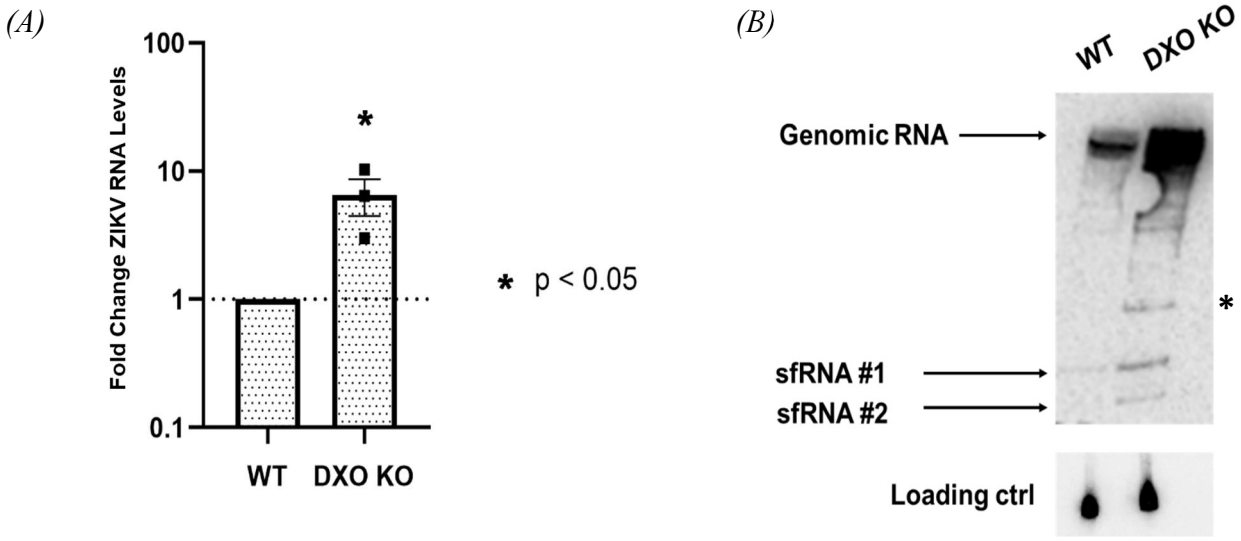

Figure 5. Quantification of ZIKV RNA abundance in WT vs. DXO KO cells. (A) Digital PCR Quantification of Relative Intracellular ZIKV RNA Abundance in WT and DXO KO Cells. Total RNA was extracted from infected HEK cells 72 hpi. Primers specific to the ZIKV genome were used to quantify relative abundance of ZIKV RNA present in WT and DXO KO cells. *(B)* Northern Blots of ZIKV Genomic RNA. Total RNA extracted was resolved on a 5% denaturing polyacrylamide gel and transferred to a nylon membrane for subsequent probing of viral RNA. Probes used were specific to the ZIKV 3' UTR. One extra band that has not yet been identified appeared in the DXO KO cell line and has been labeled with an asterisk.

northern blot using probes against the ZIKV 3' UTR (Figure 6B). Visually there is an apparent increase in viral genome abundance in the DXO KO cells compared to WT cells. We conclude that DXO represses viral replication during ZIKV infection. In addition to the visual increase in viral RNA abundance, an extra band appears above the two sfRNAs. This larger viral RNA is currently unidentified but may suggest that DXO is necessary to degrade this RNA. Therefore in cells lacking DXO, the RNA decay pathway may be stalling on a certain area of the viral genome and thus creating a new decay intermediate.

DXO Helps Maintain Sustained High Viral Titers During Flavivirus Infection

Based on the previous set of data, we wanted to examine if the increase in viral RNA abundance translated to an increase in viral titers. Additionally, we wanted to assess the growth kinetics of different viruses in the presence and absence of DXO in order to see if similar phenotypes are observed across the flavivirus genus. YFV and KUNV were used to infect WT and DXO KO cells at a MOI of 0.01. Infectious media was collected at each timepoint and viral titers were quantified by focus forming assays, as previously described[79]. YFV showed approximately a one-log increase in viral titers in DXO KO cells compared to WT cells on days two through four (Figure 7). Interestingly, there was no difference in KUNV titers observed during the exponential phase of viral growth. Both YFV and KUNV displayed a drastic decrease in viral titer starting on day five and four, respectively. These results suggest that DXO represses YFV replication. Images of the cells during KUNV infection were taken to observe for cytopathic effects (CPE). On day four post-infection, DXO KO cells showed significant signs of CPE and were not adhered to the flask while WT cells appeared alive. Visually the data suggests that cells lacking DXO undergo increased CPE during viral infection compared to cells containing DXO, suggesting that DXO may help maintain cell viability during infection.

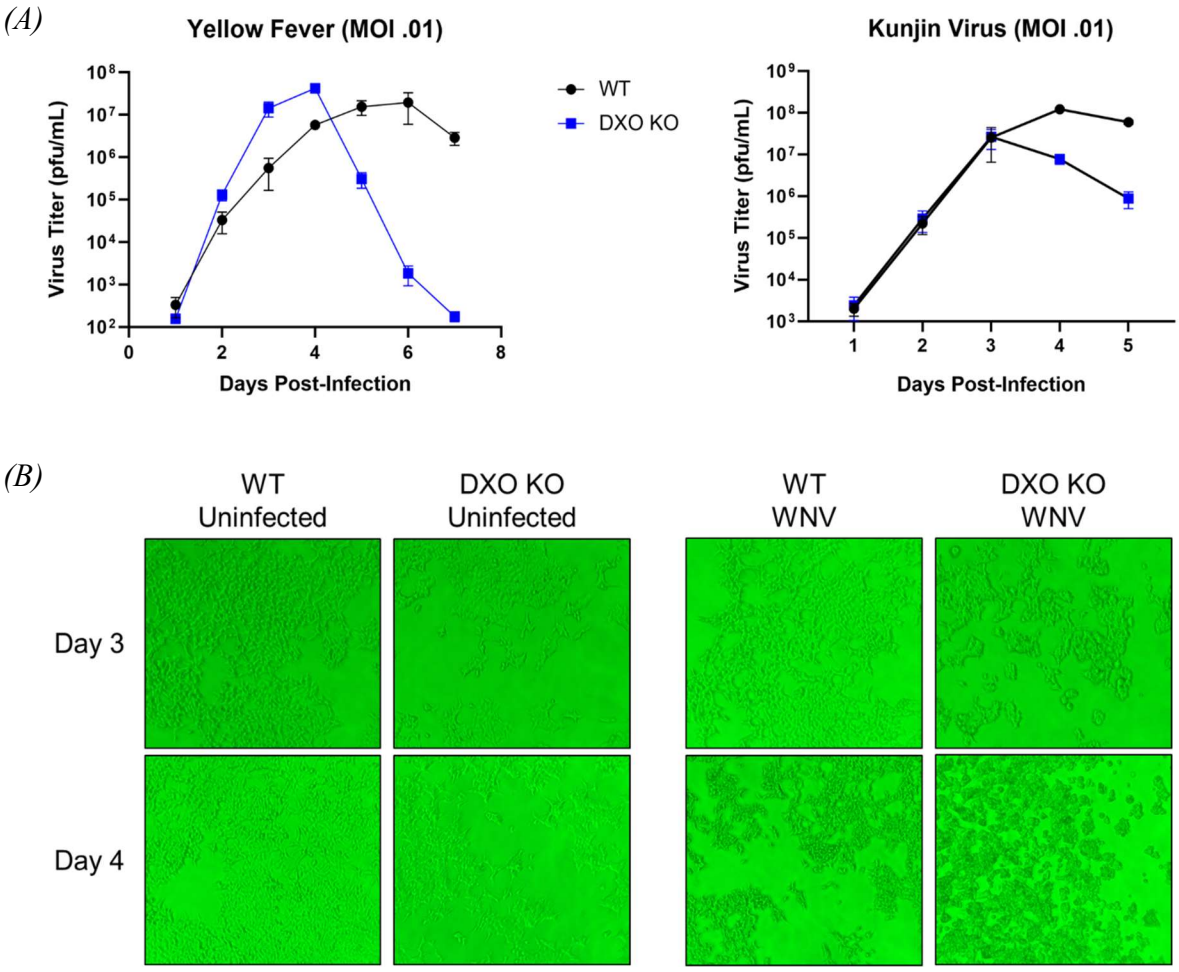

Figure 6. DXO affects the replication of YFV and maintains sustained high viral titers in YFV and KUNV. (A) YFV and KUNV titers in WT and DXO KO cell media infected with a MOI of 0.01. Infectious media from each timepoint was analyzed using a focus forming assay. The average pfu/mL of each timepoint was plotted over time with error bars representing standard error of the mean. *(B)* Microscope images of WT and DXO KO cells infected with KUNV three- and four-days post-infection. Images of uninfected and infected cell lines are displayed.

DXO Reduces Sindbis Virus Growth and Viral RNA Accumulation

We next wanted to determine if DXO affects positive-strand RNA viruses of a different genus from flaviviruses and thus selected the alphavirus, SINV. WT and DXO KO cells were infected with SINV at a MOI of 0.01 and media as well as cellular RNA was collected at each timepoint. Viral titers were quantified through plaque assays using the infectious media

collected. SINV titers were significantly higher in DXO KO cells compared to WT cells at twelve through forty-eight hours post-infection (Figure 7). Increases in both intracellular and

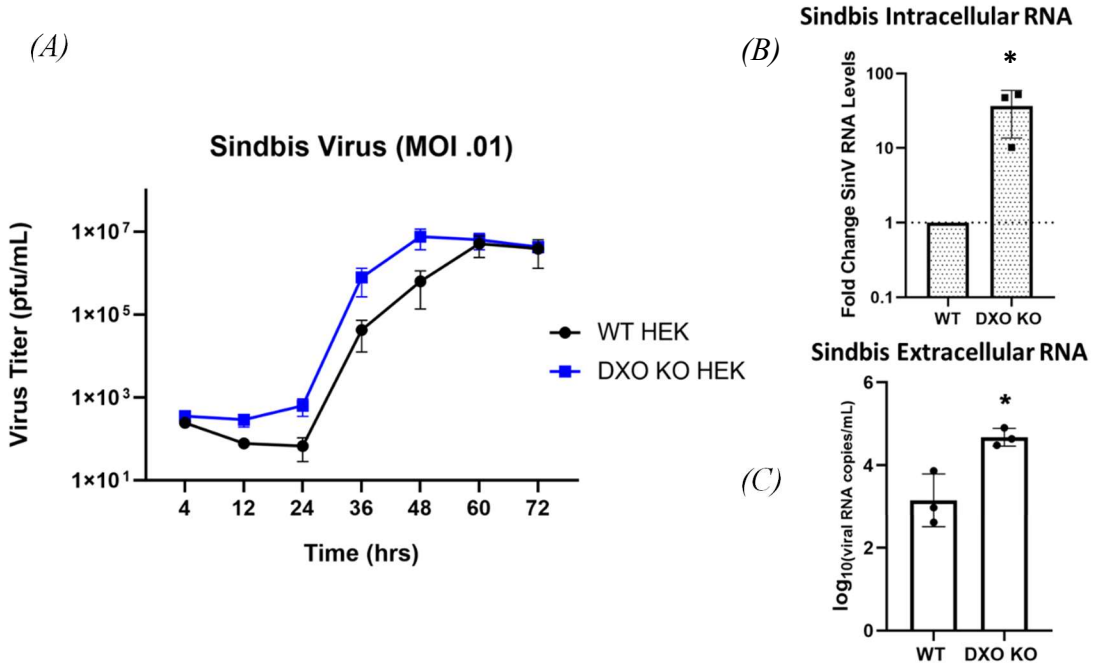

Figure 7. DXO represses SINV replication. (A) SINV titers in WT and DXO KO cell media infected with a MOI of 0.01. Infectious media from each timepoint was analyzed using a focus forming assay. The average pfu/mL of each timepoint was plotted over time with error bars representing standard error of the mean. *(B)* Fold change of SINV intracellular RNA abundance 48 hpi. Total RNA was extracted from infected HEK cells. Primers specific to the SINV genome were used to quantify relative viral RNA abundance in WT and DXO KO cells using digital droplet PCR. *(C)* Digital droplet PCR quantification of extracellular viral RNA 48 hpi. Total RNA was extracted from infectious media and primers specific to the SINV genome were used to quantify viral RNA copies/mL.

extracellular viral RNA were observed in DXO KO cells compared to WT cells at forty-eight hours post-infection. We conclude that DXO represses SINV replication thus leading to decreased viral titers.

What are the Potential Mechanisms Behind DXO as an Antiviral Effector?

Previous studies have shown that mRNA 5' caps that are 2'-O-methylated are protected from DXO degradation[47]. Because flavivirus genomes contain a 2'-O-methylation in their 5'

caps, this potentially provides the viral RNA with a disguise to evade degradation by DXO. In order to further investigate, a mutant E218A KUNV was constructed that prevents the virus from 2'-O-methylating the 5' cap during replication of the genome[74]. This mutant virus was used to infect both WT and DXO KO cells at a MOI of 0.01 and infectious media was collected to quantify viral titer. No difference was observed in E218A KUNV replication rates between the WT and DXO KO cells (Figure 8) during the exponential phase of growth, although a reduction of titer was observed at days 4 and 5 in DXO KO cells compared to WT. Overall, the growth kinetics of the E218A mutant KUNV is very similar to that of the WT KUNV (Figure 8). We conclude that no differences were observed between WT and DXO KO cells as well as WT and E218A KUNV through growth kinetics. Intracellular viral RNA abundance might display a more comprehensive mechanistic picture than released viral titers and thus we cannot rule out that 2'-O-methlyation of the first transcript base may still play a role in DXO evasion.

The well-known exonuclease, XRN1, stalls on highly structured 3' UTR pseudoknots thus creating sfRNAs[65]. In collaboration with Phillida Charley in the Wilusz lab, we wanted to

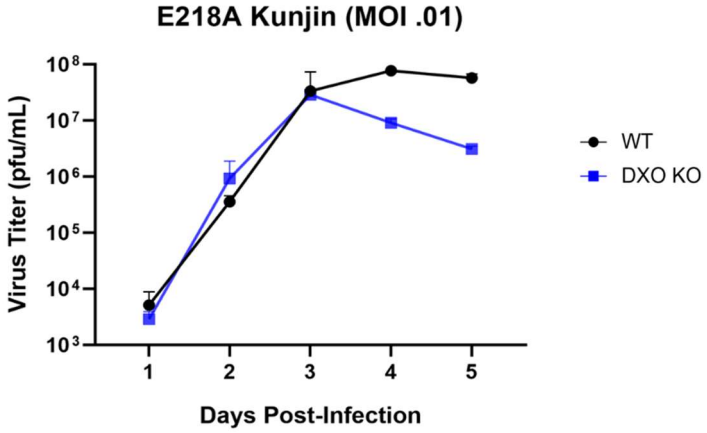

Figure 8. KUNV lacking 2'-O-methlyation on the first base of the transcript does not affect viral growth kinetics in WT and DXO KO cells. WT and DXO KO cells were infected at a MOI of .01 with E218A KUNV. Infectious media was collected and analyzed using a focus forming assay. The average pfu/mL was plotted over time and the error bars represent standard error of the mean.

examine if DXO also stalls on these RNA structures to produce sfRNAs or if it degrades through the pseudoknots. Radiolabeled 3' UTRs of DENV and the phlebovirus, Rift Valley fever virus (RVFV), were incubated with XRN1 and DXO under established conditions for each enzyme. Viral RNA products were examined on a polyacrylamide gel using phosphorescence. XRN1 creates two decay intermediates on the DENV-2 3' UTR and one decay intermediate on RVFV-N that appeared after one minute of incubation (Figure 9). No apparent bands appeared after DXO was added to the 3' UTRs, thus suggesting no decay intermediates were generated by the action of the enzyme. We conclude that DXO does not stall on pseudoknots located on the 3' UTR of RNA viruses.

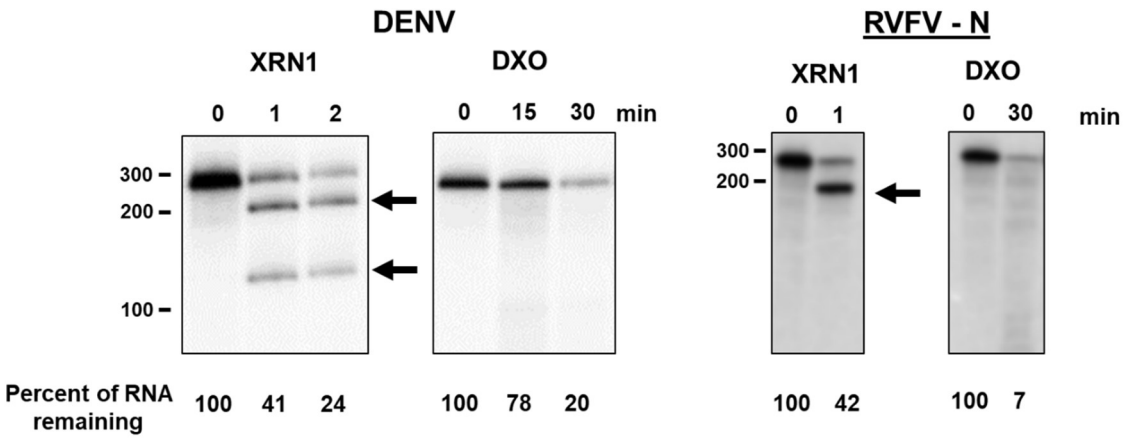

Figure 9. Mammalian DXO does not create decay intermediates. Data generated in collaboration with Dr. Phillida Charley, Dr. Jeff Wilusz Lab. The 3' UTRs of DENV-2 and RVFV-N were radiolabeled using α-32P- UTP and used as substrates for recombinant XRN1 and DXO. Arrows point to decay intermediates observed. Samples were taken at timepoints listed above the gel. The percentage of RNA remaining at timepoints taken during the reactions are listed below relative to the starting RNA substrate abundance labeled as 100%. The sizes of the starting RNA and the decay intermediates produced are indicated on the left.

Discussion

As flaviviruses and alphaviruses continue to threaten populations across the globe, the need for effective vaccines and antiviral therapeutics grows stronger. By understanding the details behind viral interactions with the cellular environment during infection, we can shed light on various targets for preventative care and treatments. Recent studies have demonstrated the critical roles of the RNA decay pathway during viral infections. XRN1 is the most well-known of the 5' to 3' exonucleases to be involved in degrading viral RNAs but stalls on pseudoknot-containing three helix junction structures located in certain viral 3' UTRs[65]. Stalling of XRN1 subsequently leads to dysregulation of mRNA transcripts, decrease in cellular responses to the viral infection, and formation of sfRNAs during flavivirus infection[80]. In this study we evaluated the effect of the decapping 5' to 3' exoribonuclease, DXO, on flavivirus and alphavirus replication.

There are few publications focused on the mammalian DXO and its general role within the cell. Previous publications have shown that the decapping 5' to 3' exonuclease is a nuclear protein in HeLa and U2OS cancer cell lines[47,75]. HEK cells were used in these studies however no information has been published on DXO localization in HEK cells. A nuclear-cytoplasmic fractionation was performed on the HEK cell line and analyzed using a western blot. This study showed that DXO is a cytoplasmic protein in HEK cells unlike in HeLa or U2OS cell lines. Our findings suggest that DXO is differentially localized in various cell lines. In addition, genomes of RNA viruses replicate within the cytoplasm during infection and therefore it is plausible for DXO to target the foreign RNAs for degradation. Based on our data, HeLa cell DXO may not affect viral RNA unless the exonuclease translocates from the nucleus to the cytoplasm during infections. To further understand the antiviral functions of DXO in HEK cells as well as in

different cell lines, it would be interesting to investigate viral replication rates in HeLa cells and HeLa DXO KO cells.

In order to study the effects of DXO on RNA virus replication, a CRISPR-based DXO knockout cell line in HEK cells was obtained through our collaborator, Mike Kiledjian, at Rutgers University[48]. We wanted to examine if there were any noticeable phenotypes in cells lacking DXO compared to WT cells that may affect further experiments. Overall results showed the two cell lines had similar growth rates. The DXO KO cell line did however appear to display a lag in growth which may be due to the mutant cell line's inability to adhere quickly to the flask and respond to stress such as passaging of the cells. We concluded that the minor lag observed in DXO KO cell growth will not affect further experimentation and the overall growth rate is comparable to that of WT cells. Overall the lack of DXO should not affect cell growth or the accuracy of the results. Certain proteins are essential for cell survival and upon knocking out the protein, dysregulation occurs within the cell and may lead to a decreased cell viability. The data we have observed comparing WT and DXO KO cells suggests that the minor lag in growth will not interfere with further experimentation with viral infections.

Subsequent experiments infected WT and DXO KO cells with various flaviviruses to analyze the effects of DXO on viral replication. We found that following infection with ZIKV at a high MOI, intracellular viral RNA was significantly increased 72 h post-infection in DXO KO cells compared to WT cells. Interestingly, the Northern blot showed there was also an increase in intensity of sfRNA#1 and #2 in DXO KO cells compared to WT. The increase in sfRNA abundance within the cell could lead to increased cell dysregulation due as the decay intermediates sequester essential cellular proteins. The observed increase in decay intermediates formed in cells lacking DXO suggests that the decapping exonuclease may play a role in

degrading sfRNAs while XRN1 stalls on such structures. In addition to the observed increase in sfRNAs, an additional band appears above the two known decay intermediates. This band is larger than the two sfRNAs and suggests that without DXO, the RNA decay pathway stalls on a different area of the ZIKV viral RNA thus creating a new decay intermediate. It is possible that DXO works with XRN1 to overcome and degrade highly structured areas of the flavivirus RNA. Through understanding where on the viral genome the decay intermediate is forming, we can better comprehend the role DXO plays in aiding viral RNA degradation. Overall this experiment shows that DXO plays a role in suppressing flavivirus replication within the cell. Further experimentation with other flaviviruses is necessary to understand if the phenotype observed is ZIKV or flavivirus specific.

Growth kinetics of YFV and KUNV were analyzed in WT and DXO KO cells infecting with a lower MOI to better observe minor differences between the two cell lines. Over the course of the first few days there is a significant increase in YFV viral titers from DXO KO cell compared to WT cells while no difference is observed in KUNV titers. The growth kinetics suggest that DXO has an effect on YFV by reducing the viral titers but does not appear to influence the abundance of KUNV virions. In addition, infections using different viruses of the same genus do not seem to have the same phenotype in the presence and absence of DXO.

Curiously, both YFV and KUNV growth curves display a drastic decrease in viral titers on day five and four, respectively. The reasoning behind this reduction in both titers cannot yet be fully explained however, an increase in cytopathic effect and cell death was observed in DXO KO cells but not in WT cells on the days the titers decreased rapidly. This phenotype was observed microscopically and additional experiments are necessary to analyze apoptosis and necrosis incidences in both cell lines during infections. The increase in cytopathic effect may be

due to the unfolded protein response (UPR). Previous research has shown accumulation of unfolded flavivirus proteins on the endoplasmic reticulum (ER) induces stress and the UPR[81]. Too much accumulation of unfolded proteins on the ER can lead to significant dysregulation of translation machinery and cellular homeostasis, thus leading to rapid cell death. As our data has shown, there is a significant increase in intracellular flavivirus RNA in DXO KO cells which may lead to an increase in polyproteins on the ER and cell death due to dysregulation of host machinery. In order to test if the UPR is being induced, one could first analyze if an increase in expression of UPR components such as kinases and an increase in viral proteins occurs during infection through a Western blot. Based on our data, we hypothesize that UPR components will be greatly expressed in DXO KO cells and not WT cells during infection since an increase in viral RNA in the knockout cell line would potentially lead to a significant increase in unfolded polyprotein. If we observe such results, this will indicate that the increase in viral proteins may be inducing the UPR thus leading to cellular dysregulation and cell death. In addition, our data also has shown an increase in sfRNA during flavivirus infection in DXO KO cells. Previous studies have shown that sfRNA can function as a protein sponge within the cell by binding a multitude of important factors such as those involved in splicing, the RNA decay pathway, and the innate type I IFN response[80]. An increase in the accumulation of sfRNAs as seen in DXO KO cells may lead to a greater imbalance in mechanisms of cellular regulation and rapid cell death.

Our data shows that flaviviruses are affected by DXO but we wanted to test if other positive-strand RNA viruses of a different genus were influenced by the decapping exonuclease during infection. Results show that the amount of infectious SINV released from cells was significantly increased in DXO KO cells compared to WT cells and there was a corresponding increase in extracellular viral RNA as well. This study suggests that DXO reduces the abundance

of infectious SINV virus being released from the cell and can be confirmed through the reduction in extracellular SINV RNA. Additionally, intracellular SINV RNA was increased in the absence of DXO. Altogether, we can conclude that DXO plays a significant role in suppressing the overall replication of SINV through reducing the abundance of intracellular RNA and thus reducing viral titer. This study suggests that DXO affects the replication of positive-strand RNA viruses of different genera however a more extensive variety of RNA viruses must be tested in the presence and absence of DXO.

Thus far we have shown that DXO plays a role in positive-strand RNA virus replication, but the mechanistic details behind the exonuclease have yet to be uncovered. As positive-strand RNA viral genomes localize within the cytoplasm, it is critical for these RNAs to have a method of evading DXO degradation. Shedding light on how flaviviruses and alphaviruses evade DXO will also elucidate how they are targeted by DXO. A recent publication from a collaboration between the Geiss and Bisaillon labs shown that 2'-O-methylation of the 5' cap can protect mRNAs from DXO degradation[47]. Interestingly, flaviviruses have evolved to have a 2'-O-methylated 5' cap that has been shown to help evade cellular sensing molecules such as IFIT, and the presence of 2'O-methylation on flavivirus genomes could provide a potential mechanism of eluding the decapping exonuclease[74]. Additionally, alphaviruses do not have 2'-O-methylated 5' caps but may use a different means of DXO evasion. In order to further examine if 2'-O-methylation protects flaviviruses from DXO degradation, an E218A mutant of KUNV was constructed and used to infect WT and DXO KO cells. Growth kinetics of the mutant virus were similar to that of the wildtype KUNV. Due to wildtype KUNV not displaying a difference in growth rates between WT and DXO KO cells, analyzing if the lack of 2'-O-methylation affects viral titer is not possible. However, it is possible that 2'-O-methylation may play a role in

protecting other flavivirus genomes that show different growth rates in DXO KO cells (such as YF). The differences in RNA structures between flaviviruses and alphaviruses may explain why there are differences in growth kinetics in the presence and absence of DXO. Further experimentation mutating 2'-O-methylation or RNA structures in other viruses such as YFV or ZIKV may provide more insight and display more of a change in growth rates compared to the wildtype viruses.

Based on the decapping and 5' to 3' exonuclease activity of DXO, we hypothesized that DXO can degrade capped viral RNA but may stall on the 3' UTR pseudoknots similar to XRN1. Previous data has shown that yeast DXO does create decay intermediates when added to various positive-stranded plant virus and mosquito-borne flavivirus RNA[82,83]. However, the yeast DXO used in the published data is a weak homolog of the mammalian DXO used in our studies. To understand how DXO interacts with viral RNAs, 3' UTRs of DENV and RVFV were radiolabeled and incubated with the exonuclease. XRN1 was used as a positive control as it is well-known the exonuclease stalls on the pseudoknots of viral 3' UTRs. As expected, XRN1 created two RNA decay intermediates when incubated with DENV and one decay intermediate appeared with RVFV. Interestingly, no decay intermediates formed when the same viral 3' UTRs were incubated with DXO. Our data suggests that DXO does not stall on the pseudoknots like XRN1 and has the ability to degrade sfRNAs during flavivirus infection. We previously showed cells lacking DXO display an increase in genomic and sfRNA abundance during flavivirus infection. Altogether, the increase in sfRNA may explain the increase in cytopathic effect and rapid cell death in the absence of DXO during infection. Additional experimentation using radiolabeled 5' UTRs or whole viral genomes may show if DXO stalls on different areas of viral

genomes. It is possible that DXO and XRN1 work together to pick up the degradation slack when one or the other stall.

Overall the goal of these studies was to elucidate the role of DXO during positive-strand RNA virus infection. Results show that DXO does affect certain viruses such as ZIKV and YFV by suppressing their replication however, there are viruses of the same flavivirus genus such as KUNV that do not appear to be influenced by DXO. Our data suggests that DXO reduces the abundance of viral RNA intracellularly and extracellularly during ZIKV and YFV infections leading to a reduction in viral titers. Additionally, we demonstrated that DXO does affect the replication of positive-strand RNA viruses of other genera through showing a decrease in intracellular and extracellular SINV RNA and viral titer occurs in the presence of DXO. Mechanisms of DXO may include targeting viral RNAs through the lack of 2'-O-methlyation in the 5' cap however we observed no difference in the wildtype KUNV growth kinetics compared to the E218A KUNV. Results also suggested that DXO does not stall on pseudoknots of the 3' UTR like XRN1 and therefore can degrade sfRNAs during flavivirus infection.

Future experimentation is necessary for beginning to understand DXO's role as an RNA virus restriction factor. In order to show that DXO is responsible for the effects on viral growth, we have constructed a plasmid to re-express DXO in the DXO KO cell line. We hypothesize that by infecting knockout cells that have been transfected with the DXO expression plasmid, we will see a decrease in viral titers and RNA abundance comparable to what we have observed in WT cells. These experiments have yet to be completed but the plasmid expressing DXO has been constructed. In addition, we plan on investigating changes in intracellular and extracellular viral RNA during each infection such as what we have shown with SINV. Although KUNV did not display a change in viral growth kinetics during infection of WT and DXO KO cells, we did

observe a rapid reduction in viral titers a few days post-infection. KUNV may have more of an intracellular effect in WT and DXO KO cells and analyzing abundance of viral RNA could determine if DXO is reducing viral genome copies. Due to the lack of change observed in wildtype and E218A KUNV titers in WT and DXO KO cells, we also plan to make a similar mutation using YFV or ZIKV where the titers are noticeably different. Next, as we have shown DXO does not stall on viral 3' UTR structures, we would like to examine the exonuclease's ability to degrade viral 5' UTRs. There may be structures that stall DXO but not XRN1, potentially making it crucial for the two 5' to 3' exonucleases to work together to degrade viral RNAs. Finally, the growth kinetics vary from virus to virus but this inconsistency may be explained through adaptation of the DXO KO cell line. Recently it has been published that knockout cell lines over time can compensate for the loss of protein function through differentially expressing other genes[84]. In order to test if the DXO KO cell line has adapted to the loss of DXO, we plan on comparing viral RNA abundances through infecting DXO KO and knockdown (DXO KD) cells. Knockdown cells will be made through transfecting WT HEK cells with siRNAs specific to DXO. If we observe significant differences between the DXO KO and DXO KD cells then this may be indicative of the knockout cells having adapted and we will need to change our methods to using knockdown cells.

To summarize, we concluded that the decapping 5' to 3' exonuclease can influence the replication of certain positive-strand RNA viruses. Due to the lack previous research regarding mechanisms of DXO in the cell and during viral infections, this data represents the first steps towards understanding DXO's potential role as a novel antiviral factor. These studies warrant further experimentation to comprehend the mechanisms of DXO as well as how virus growth kinetics are affected in the presence or absence of DXO.

References

1. Saeedi, B. J. & Geiss, B. J. Regulation of flavivirus RNA synthesis and capping. *Wiley Interdisciplinary Reviews: RNA* (2013). doi:10.1002/wrna.1191

2. Packard, R. M. The Fielding H. Garrison Lecture: "Break-Bone" Fever in Philadelphia, 1780: Reflections on the History of Disease. *Bull. Hist. Med.* (2016). doi:10.1353/bhm.2016.0041

3. Muller, D. A., Depelsenaire, A. C. I. & Young, P. R. Clinical and laboratory diagnosis of dengue virus infection. *J. Infect. Dis.* (2017). doi:10.1093/infdis/jiw649

4. Sangkawibha, N. *et al.* Risk factors in dengue shock syndrome: A prospective epidemiologic study in Rayong, Thailand: I. THE 1980 outbreak. *Am. J. Epidemiol.* (1984). doi:10.1093/oxfordjournals.aje.a113932

5. Screaton, G., Mongkolsapaya, J., Yacoub, S. & Roberts, C. New insights into the immunopathology and control of dengue virus infection. *Nature Reviews Immunology* (2015). doi:10.1038/nri3916

6. Plourde, A. R. & Bloch, E. M. A literature review of zika virus. *Emerging Infectious Diseases* (2016). doi:10.3201/eid2207.151990

7. Araujo, A. Q. C., Silva, M. T. T. & Araujo, A. P. Q. C. Zika virus-associated neurological disorders: A review. *Brain* (2016). doi:10.1093/brain/aww158

8. Paixão, E. S., Barreto, F., Da Glória Teixeira, M., Da Conceição N Costa, M. & Rodrigues, L. C. History, epidemiology, and clinical manifestations of Zika: A systematic review. *American Journal of Public Health* (2016). doi:10.2105/AJPH.2016.303112

9. Chippaux, J. P. & Chippaux, A. Yellow fever in Africa and the Americas: A historical and epidemiological perspective. *Journal of Venomous Animals and Toxins Including Tropical Diseases* (2018). doi:10.1186/s40409-018-0162-y

10. Barnett, E. D. Yellow Fever: Epidemiology and Prevention. *Clin. Infect. Dis.* (2007). doi:10.1086/511869

11. Meegan, J. M. Yellow fever. in *Handbook of Zoonoses, Second Edition, Section B: Viral Zoonoses* (2017). doi:10.1201/9780203752463

12. Shearer, F. M. *et al.* Global yellow fever vaccination coverage from 1970 to 2016: an adjusted retrospective analysis. *Lancet Infect. Dis.* (2017). doi:10.1016/S1473-3099(17)30419-X

13. Luedtke, P. & Greenlee, J. E. West nile virus. in *Handbook of Peripheral Neuropathy* (2005).

14. Suthar, M. S., Diamond, M. S. & Gale, M. West Nile virus infection and immunity. *Nature Reviews Microbiology* (2013). doi:10.1038/nrmicro2950

15. Petersen, L. R., Brault, A. C. & Nasci, R. S. West Nile virus: Review of the literature. *JAMA - Journal of the American Medical Association* (2013). doi:10.1001/jama.2013.8042

16. da Cunha, R. V. & Trinta, K. S. Chikungunya virus: Clinical aspects and treatment. *Memorias do Instituto Oswaldo Cruz* (2017). doi:10.1590/0074-02760170044

17. Pialoux, G., Gaüzère, B. A., Jauréguiberry, S. & Strobel, M. Chikungunya, an epidemic arbovirosis. *Lancet Infectious Diseases* (2007). doi:10.1016/S1473-3099(07)70107-X

18. Weaver, S. C., Osorio, J. E., Livengood, J. A., Chen, R. & Stinchcomb, D. T. Chikungunya virus and prospects for a vaccine. *Expert Review of Vaccines* (2012). doi:10.1586/erv.12.84

19. Burt, F. J. *et al.* Chikungunya virus: an update on the biology and pathogenesis of this emerging pathogen. *The Lancet Infectious Diseases* (2017). doi:10.1016/S1473-3099(16)30385-1

20. Esposito, D. L. A. & Fonseca, B. A. L. da. Will Mayaro virus be responsible for the next outbreak of an arthropod-borne virus in Brazil? *Brazilian Journal of Infectious Diseases* (2017). doi:10.1016/j.bjid.2017.06.002

21. Acosta-Ampudia, Y. *et al.* Mayaro: an emerging viral threat? *Emerging Microbes and Infections* (2018). doi:10.1038/s41426-018-0163-5

22. Calisher, C. H., Gutierrez, E., Maness, K. S. C. & Lord, R. D. Isolation of Mayaro virus from a migrating bird captured in Louisiana in 1967. *Bull. Pan Am. Health Organ.* (1974).

23. Sharma, A. & Knollmann-Ritschel, B. Current understanding of the molecular basis of venezuelan equine encephalitis virus pathogenesis and vaccine development. *Viruses* (2019). doi:10.3390/v11020164

24. Kinney, R. M. *et al.* Attenuation of Venezuelan equine encephalitis virus strain TC-83 is encoded by the 5'-noncoding region and the E2 envelope glycoprotein. *J. Virol.* (1993).

25. Paessler, S. & Weaver, S. C. Vaccines for Venezuelan equine encephalitis. *Vaccine* (2009). doi:10.1016/j.vaccine.2009.07.095

26. Garcia-Blanco, M. A., Vasudevan, S. G., Bradrick, S. S. & Nicchitta, C. Flavivirus RNA

transactions from viral entry to genome replication. *Antiviral Research* (2016). doi:10.1016/j.antiviral.2016.09.010

27. Silva, L. A. & Dermody, T. S. Chikungunya virus: Epidemiology, replication, disease mechanisms, and prospective intervention strategies. *Journal of Clinical Investigation* (2017). doi:10.1172/JCI84417

28. Liu, L. Fields Virology, 6th Edition. *Clin. Infect. Dis.* (2014). doi:10.1093/cid/ciu346

29. Roby, J. A., Setoh, Y. X., Hall, R. A. & Khromykh, A. A. Post-translational regulation and modifications of flavivirus structural proteins. *Journal of General Virology* (2015). doi:10.1099/vir.0.000097

30. Hyde, J. L. *et al.* A viral RNA structural element alters host recognition of nonself RNA. *Science (80-.).* (2014). doi:10.1126/science.1248465

31. Cross, S. T., Michalski, D., Miller, M. R. & Wilusz, J. RNA regulatory processes in RNA virus biology. *Wiley Interdisciplinary Reviews: RNA* (2019). doi:10.1002/wrna.1536

32. Issur, M. *et al.* The flavivirus NS5 protein is a true RNA guanylyltransferase that catalyzes a two-step reaction to form the RNA cap structure. *RNA* (2009). doi:10.1261/rna.1609709

33. Delorme-Axford, E. & Klionsky, D. J. On the edge of degradation: Autophagy regulation by RNA decay. *Wiley Interdiscip. Rev. RNA* (2019). doi:10.1002/wrna.1522

34. Chávez, S., García-Martínez, J., Delgado-Ramos, L. & Pérez-Ortín, J. E. The importance of controlling mRNA turnover during cell proliferation. *Current Genetics* (2016). doi:10.1007/s00294-016-0594-2

35. Yamashita, A. *et al.* Concerted action of poly(A) nucleases and decapping enzyme in mammalian mRNA turnover. *Nat. Struct. Mol. Biol.* (2005). doi:10.1038/nsmb1016

36. Gagliardi, D. & Dziembowski, A. 50 and 30 modifications controlling RNA degradation: From safeguards to executioners. *Philos. Trans. R. Soc. B Biol. Sci.* (2018). doi:10.1098/rstb.2018.0160

37. Heck, A. M. & Wilusz, J. The interplay between the RNA decay and translation machinery in eukaryotes. *Cold Spring Harb. Perspect. Biol.* (2018). doi:10.1101/cshperspect.a032839

38. De Almeida, C., Scheer, H., Zuber, H. & Gagliardi, D. RNA uridylation: a key posttranscriptional modification shaping the coding and noncoding transcriptome. *Wiley Interdisciplinary Reviews: RNA* (2018). doi:10.1002/wrna.1440

39. Yi, H. *et al.* PABP Cooperates with the CCR4-NOT Complex to Promote mRNA Deadenylation and Block Precocious Decay. *Mol. Cell* (2018). doi:10.1016/j.molcel.2018.05.009

40. Munoz-Tello, P., Rajappa, L., Coquille, S. & Thore, S. Polyuridylation in eukaryotes: A 3′-end modification regulating RNA life. *BioMed Research International* (2015). doi:10.1155/2015/968127

41. Topisirovic, I., Svitkin, Y. V., Sonenberg, N. & Shatkin, A. J. Cap and cap-binding proteins in the control of gene expression. *Wiley Interdisciplinary Reviews: RNA* (2011). doi:10.1002/wrna.52

42. SGrudzien-Nogalska, E. & Kiledjian, M. New insights into decapping enzymes and

selective mRNA decay. *Wiley Interdisciplinary Reviews: RNA* (2017). doi:10.1002/wrna.1379

43. Arribas-Layton, M., Wu, D., Lykke-Andersen, J. & Song, H. Structural and functional control of the eukaryotic mRNA decapping machinery. *Biochimica et Biophysica Acta - Gene Regulatory Mechanisms* (2013). doi:10.1016/j.bbagrm.2012.12.006

44. Chowdhury, A., Kalurupalle, S. & Tharun, S. Pat1 contributes to the RNA binding activity of the Lsm1-7-Pat1 complex. *RNA* (2014). doi:10.1261/rna.045252.114

45. Sachdev, R. *et al.* Pat1 promotes processing body assembly by enhancing the phase separation of the DEAD-box ATPase Dhh1 and RNA. *Elife* (2019). doi:10.7554/eLife.41415

46. Lu, G. *et al.* hNUDT16: A universal decapping enzyme for small nucleolar RNA and cytoplasmic mRNA. *Protein Cell* (2011). doi:10.1007/s13238-011-1009-2

47. Picard-Jean, F. *et al.* 2'-O-methylation of the mRNA cap protects RNAs from decapping and degradation by DXO. *PLoS One* (2018). doi:10.1371/journal.pone.0193804

48. Jiao, X. *et al.* 5′ End Nicotinamide Adenine Dinucleotide Cap in Human Cells Promotes RNA Decay through DXO-Mediated deNADding. *Cell* (2017). doi:10.1016/j.cell.2017.02.019

49. Wang, Z., Jiao, X., Carr-Schmid, A. & Kiledjian, M. The hDcp2 protein is a mammalian mRNA decapping enzyme. *Proc. Natl. Acad. Sci.* (2002). doi:10.1073/pnas.192445599

50. Peng, Y. & Schoenberg, D. R. c-Src Activates Endonuclease-Mediated mRNA Decay. *Mol. Cell* (2007). doi:10.1016/j.molcel.2007.01.026

51. Wang, Z. & Kiledjian, M. Identification of an erythroid-enriched endoribonuclease activity involved in specific mRNA cleavage. *EMBO J.* (2000). doi:10.1093/emboj/19.2.295

52. Schoenberg, D. R. & Maquat, L. E. Regulation of cytoplasmic mRNA decay. *Nature Reviews Genetics* (2012). doi:10.1038/nrg3160

53. Gallouzi, I. *et al.* A Novel Phosphorylation-Dependent RNase Activity of GAP-SH3 Binding Protein: a Potential Link between Signal Transduction and RNA Stability. *Mol. Cell. Biol.* (2015). doi:10.1128/mcb.18.7.3956

54. Schoenberg, D. R. Mechanisms of endonuclease-mediated mRNA decay. *Wiley Interdisciplinary Reviews: RNA* (2011). doi:10.1002/wrna.78

55. Meister, G. *et al.* Human Argonaute2 mediates RNA cleavage targeted by miRNAs and siRNAs. *Mol. Cell* (2004). doi:10.1016/j.molcel.2004.07.007

56. Chlebowski, A., Lubas, M., Jensen, T. H. & Dziembowski, A. RNA decay machines: The exosome. *Biochimica et Biophysica Acta - Gene Regulatory Mechanisms* (2013). doi:10.1016/j.bbagrm.2013.01.006

57. Orban, T. I. & Izaurralde, E. Decay of mRNAs targeted by RISC requires XRN1, the Ski complex, and the exosome. *RNA* (2005). doi:10.1261/rna.7231505

58. Kowalinski, E. *et al.* Structure of a Cytoplasmic 11-Subunit RNA Exosome Complex. *Mol. Cell* (2016). doi:10.1016/j.molcel.2016.05.028

59. łabno, A. *et al.* Perlman syndrome nuclease DIS3L2 controls cytoplasmic non-coding RNAs and provides surveillance pathway for maturing snRNAs. *Nucleic Acids Res.*

(2016). doi:10.1093/nar/gkw649

60. Łabno, A., Tomecki, R. & Dziembowski, A. Cytoplasmic RNA decay pathways - Enzymes and mechanisms. *Biochimica et Biophysica Acta - Molecular Cell Research* (2016). doi:10.1016/j.bbamcr.2016.09.023

61. Sun, M. *et al.* Global analysis of Eukaryotic mRNA degradation reveals Xrn1-dependent buffering of transcript levels. *Mol. Cell* (2013). doi:10.1016/j.molcel.2013.09.010

62. Haimovich, G. *et al.* XGene expression is circular: Factors for mRNA degradation also foster mRNA synthesis. *Cell* (2013). doi:10.1016/j.cell.2013.05.012

63. Fros, J. J. & Pijlman, G. P. Alphavirus infection: Host cell shut-off and inhibition of antiviral responses. *Viruses* (2016). doi:10.3390/v8060166

64. Miorin, L., Maestre, A. M., Fernandez-Sesma, A. & García-Sastre, A. Antagonism of type I interferon by flaviviruses. *Biochem. Biophys. Res. Commun.* (2017). doi:10.1016/j.bbrc.2017.05.146

65. Moon, S. L. *et al.* A noncoding RNA produced by arthropod-borne flaviviruses inhibits the cellular exoribonuclease XRN1 and alters host mRNA stability. *RNA* (2012). doi:10.1261/rna.034330.112

66. Charley, P. A. & Wilusz, J. Standing your ground to exoribonucleases: Function of Flavivirus long non-coding RNAs. *Virus Res.* (2016). doi:10.1016/j.virusres.2015.09.009

67. Schnettler, E. *et al.* Noncoding Flavivirus RNA Displays RNA Interference Suppressor Activity in Insect and Mammalian Cells. *J. Virol.* (2012). doi:10.1128/jvi.01104-12

68. Manokaran, G. *et al.* Dengue subgenomic RNA binds TRIM25 to inhibit interferon

expression for epidemiological fitness. *Science (80-.).* (2015). doi:10.1126/science.aab3369

69. Moon, S. L. *et al.* Flavivirus sfRNA suppresses antiviral RNA interference in cultured cells and mosquitoes and directly interacts with the RNAi machinery. *Virology* (2015). doi:10.1016/j.virol.2015.08.009

70. White, L. J., Wang, J. -g., Davis, N. L. & Johnston, R. E. Role of Alpha/Beta Interferon in Venezuelan Equine Encephalitis Virus Pathogenesis: Effect of an Attenuating Mutation in the 5' Untranslated Region. *J. Virol.* (2001). doi:10.1128/jvi.75.8.3706-3718.2001

71. Hyde, J. L. *et al.* The 5' and 3' ends of alphavirus RNAs - Non-coding is not non-functional. *Virus Res.* (2015). doi:10.1016/j.virusres.2015.01.016

72. Sokoloski, K. J. *et al.* Sindbis virus usurps the cellular HuR protein to stabilize its transcripts and promote productive infections in mammalian and mosquito cells. *Cell Host Microbe* (2010). doi:10.1016/j.chom.2010.07.003

73. Barnhart, M. D., Moon, S. L., Emch, A. W., Wilusz, C. J. & Wilusz, J. Changes in Cellular mRNA Stability, Splicing, and Polyadenylation through HuR Protein Sequestration by a Cytoplasmic RNA Virus. *Cell Rep.* (2013). doi:10.1016/j.celrep.2013.10.012

74. Daffis, S. *et al.* 2′-O methylation of the viral mRNA cap evades host restriction by IFIT family members. *Nature* (2010). doi:10.1038/nature09489

75. Zheng, D., Chen, C. Y. A. & Shyu, A. Bin. Unraveling regulation and new components of human P-bodies through a protein interaction framework and experimental validation.

RNA (2011). doi:10.1261/rna.2789611

76. Khromykh, A. A. & Westaway, E. G. Completion of Kunjin virus RNA sequence and recovery of an infectious RNA transcribed from stably cloned full-length cDNA. *J. Virol.* (1994).

77. Brien, J. D., Lazear, H. M. & Diamond, M. S. Propagation, quantification, detection, and storage of west nile virus. *Curr. Protoc. Microbiol.* (2013). doi:10.1002/9780471729259.mc15d03s31

78. Chang, J. H., Xiang, S., Xiang, K., Manley, J. L. & Tong, L. Structural and biochemical studies of the 5'→3' exoribonuclease Xrn1. *Nat. Struct. Mol. Biol.* (2011). doi:10.1038/nsmb.1984

79. Bullard-Feibelman, K. M. *et al.* The FDA-approved drug sofosbuvir inhibits Zika virus infection. *Antiviral Res.* (2017). doi:10.1016/j.antiviral.2016.11.023

80. Göertz, G. P., Abbo, S. R., Fros, J. J. & Pijlman, G. P. Functional RNA during Zika virus infection. *Virus Research* (2018). doi:10.1016/j.virusres.2017.08.015

81. Lewy, T. G., Grabowski, J. M. & Bloom, M. E. BiP: Master regulator of the unfolded protein response and crucial factor in flavivirus biology. *Yale Journal of Biology and Medicine* (2017).

82. Steckelberg, A. L. *et al.* A folded viral noncoding RNA blocks host cell exoribonucleases through a conformationally dynamic RNA structure. *Proc. Natl. Acad. Sci. U. S. A.* (2018). doi:10.1073/pnas.1802429115

83. MacFadden, A. *et al.* Mechanism and structural diversity of exoribonuclease-resistant

RNA structures in flaviviral RNAs. *Nat. Commun.* (2018). doi:10.1038/s41467-017-02604-y

84. El-Brolosy, M. A. & Stainier, D. Y. R. Genetic compensation: A phenomenon in search of mechanisms. *PLoS Genetics* (2017). doi:10.1371/journal.pgen.1006780